
This is an electronic reprint of the original article.
This reprint may differ from the original in pagination and typographic detail.

Pirkkalainen, Juha-Matti; Solinas, Paolo; Pekola, Jukka; Möttönen, Mikko
Non-abelian geometric phases in ground-state Josephson devices

Published in:
Physical Review B

DOI:
[10.1103/PhysRevB.81.174506](https://doi.org/10.1103/PhysRevB.81.174506)

Published: 05/05/2010

Document Version
Publisher's PDF, also known as Version of record

Please cite the original version:
Pirkkalainen, J-M., Solinas, P., Pekola, J., & Möttönen, M. (2010). Non-abelian geometric phases in ground-state Josephson devices. *Physical Review B*, 81(17), 1-4. [174506]. <https://doi.org/10.1103/PhysRevB.81.174506>

This material is protected by copyright and other intellectual property rights, and duplication or sale of all or part of any of the repository collections is not permitted, except that material may be duplicated by you for your research use or educational purposes in electronic or print form. You must obtain permission for any other use. Electronic or print copies may not be offered, whether for sale or otherwise to anyone who is not an authorised user.

Non-Abelian geometric phases in ground-state Josephson devices

J.-M. Pirkkalainen,^{1,2} P. Solinas,¹ J. P. Pekola,³ and M. Möttönen^{1,2,3}

¹*Department of Applied Physics/COMP, Aalto University, P.O. Box 15100, FI-00076 Aalto, Finland*

²*Australian Research Council Centre of Excellence for Quantum Computer Technology, School of Electrical Engineering & Telecommunications, University of New South Wales, Sydney, New South Wales 2052, Australia*

³*Low Temperature Laboratory, Aalto University, P.O. Box 13500, FI-00076 Aalto, Finland*

(Received 7 April 2010; published 5 May 2010)

We present a superconducting circuit in which non-Abelian geometric transformations can be realized using an adiabatic parameter cycle. In contrast to previous proposals, we employ quantum evolution in the ground state. We propose an experiment in which the transition from non-Abelian to Abelian cycles can be observed by measuring the pumped charge as a function of the period of the cycle. Alternatively, the non-Abelian phase can be detected using a single-electron transistor working as a charge sensor.

DOI: [10.1103/PhysRevB.81.174506](https://doi.org/10.1103/PhysRevB.81.174506)

PACS number(s): 03.65.Vf, 85.25.Dq

I. INTRODUCTION

Accurate control and measurement of few-level quantum systems has recently attracted great experimental and theoretical interest with possible applications in quantum information processing (QIP). Geometric phases¹ arising from adiabatic and cyclic quantum evolution can provide robustness against, e.g., timing errors. Recently, it was shown that such evolution in a nondegenerate ground state is immune to decoherence from a low-temperature environment² suggesting that it may provide an important tool for controlling quantum systems.

In the nondegenerate case, the accumulated geometric phase, the Berry phase,³ is a shift of the complex phase of the eigenstate and hence cannot be used as such for QIP. Non-Abelian phases^{4,5} correspond to unitary matrices operating in a degenerate subspace of the system Hamiltonian, thus providing means for universal QIP.⁶ Although geometric phases capable of entangling two quantum bits, qubits, have been observed in liquid-state nuclear magnetic resonance experiments,⁷ this kind of geometric quantum computing (GQC) is yet to be demonstrated. In fact, the geometric phases using nuclear magnetic resonance,⁷ and in more recent experiments⁸ demonstrating nonadiabatic Aharonov-Anandan phases⁹ in fullerene spin qubits, accumulate in a rotating frame, and hence there is no true degeneracy in the system.

The initial proposals for the experimental realization of GQC (Refs. 10 and 11) rely on a fully degenerate subspace to build the logical operators and it has been extended to many quantum systems^{12–14} including Josephson junction devices.^{15,16} In similar systems, a way to observe the non-Abelian evolution by measuring the charge pumped through the device has been recently proposed.¹⁷

However, all the schemes assume typically a so-called tripod Hamiltonian which has degeneracy only in its excited states [see Fig. 1(a)] rendering the system prone to decoherence even in the low-temperature limit. This is potentially a serious limitation in condensed-matter systems in which the coupling between the system and environment is strong and unavoidable.

In this paper, we present an experimentally realizable Josephson device and show that it can be used to observe adiabatic non-Abelian geometric phases. In contrast to the above

pioneering works, we employ a conceptually different Hamiltonian allowing us to work on the ground state manifold of the system. This scheme provides a clear extension to the theoretical proposals^{18–20} and experiments^{21,22} on the Berry phase in superconducting circuits.

II. NON-ABELIAN ADIABATIC EVOLUTION

We denote the parameters of the system Hamiltonian in a general cyclic loop by a vector $\vec{\lambda}$. The instantaneous eigenstates of the Hamiltonian $H[\vec{\lambda}(t)]$ along this loop for all $t \in [0, T]$ are denoted by $\{|\psi_\alpha(t)\rangle\}$, where T is the period of the cycle. Generally, any temporal evolution of the system state can be represented using the time-evolution operator, $U(T)$, such that $|\Psi(T)\rangle = U(T)|\Psi(0)\rangle$, where $|\Psi(t)\rangle$ is the state of the system at time t . The charge Q transferred through a superconducting system in a parameter cycle can be obtained by integration of the current operator $\hat{I} = -\frac{2e}{\hbar} \partial_\varphi H(t)$ as $Q = \int_0^T dt \langle \Psi(t) | \hat{I} | \Psi(t) \rangle$, where φ is the superconducting phase difference across the system.^{17,22} Using the Schrödinger equation and the definition of the time-evolution operator, this can be written in the form

$$Q = -2ie \langle \Psi(0) | U^\dagger(T) [\partial_\varphi U(T)] | \Psi(0) \rangle. \quad (1)$$

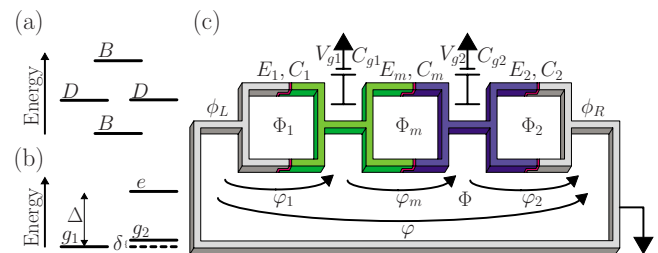


FIG. 1. (Color online) (a) Eigenenergy diagram of the so-called tripod Hamiltonian consisting of two bright states, B , and two degenerate dark states, D . (b) Eigenenergy diagram of the circuit Hamiltonian along the considered cycle. The energy difference between the ground, g , and excited, e , state is denoted by Δ and the ground state degeneracy splitting by δ . In the ideal case, $\delta=0$. (c) Circuit diagram of the non-Abelian superconducting pump. Green (left) and blue (right) denote the superconducting islands and red the Josephson junctions.

However, if the Hamiltonian parameters are changed adiabatically along the cycle, the evolution can be restricted to the initial eigenspace. In an n -fold degenerate eigenspace, the state of the system after a parameter cycle is $|\Psi(T)\rangle = U_{\text{ad}}(T)|\Psi(0)\rangle + \mathcal{O}(1/T)$, where $|\Psi(t)\rangle = \sum_{i=1}^n c_i(t)|\psi_i(t)\rangle$.⁵ If the instantaneous eigenvectors are defined globally and continuously, the operator $U_{\text{ad}}(t)$ is represented in this basis as

$$U_{\text{ad}}(t) = e^{-(i/\hbar)\int_0^t dt' E(t')} \mathcal{T} e^{-\int_0^t dt' \Gamma(t')}, \quad (2)$$

where $E(t)$ is the energy of the degenerate eigenspace, \mathcal{T} is the time-ordering operator, and the connection $\Gamma(t)$ is given by $[\Gamma(t)]_{\alpha\beta} = \langle \psi_\alpha(t) | \dot{\psi}_\beta(t) \rangle$. The first exponential function in Eq. (2) yields the accumulated dynamic phase shift, $U_{\text{dyn}}(t)$, and the second one provides the geometric transformation, $U_{\text{geo}}(t)$, which is non-Abelian, in general.

In the adiabatic limit, $U(T)$ can be replaced with $U_{\text{ad}}(T)$ and substituting Eq. (2) into Eq. (1) yields the relation between the different transformations and the transferred charge

$$Q = -2ie\{ \langle \Psi(0) | U_{\text{geo}}^\dagger(T) [\partial_\varphi U_{\text{geo}}(T)] | \Psi(0) \rangle + \langle \Psi(0) | U_{\text{dyn}}^\dagger(T) \times [\partial_\varphi U_{\text{dyn}}(T)] | \Psi(0) \rangle \}, \quad (3)$$

where the first term is the geometric pumped charge and the second one is the dynamic charge due to the usual supercurrent. In the case of a nondegenerate eigenspace, $n=1$, this reduces to the well-known relation $Q = 2e\partial_\varphi(\Theta_B - \Theta_d)$, where the accumulated Berry phase, Θ_B , is related to U_{geo} by $U_{\text{geo}} = e^{i\Theta_B}$ and the dynamic phase, Θ_d , to U_{dyn} by $U_{\text{dyn}} = e^{-i\Theta_d}$.²⁰ See Brosco *et al.*¹⁷ for an alternative way to obtain the pumped charge. Although the Berry phase induces just a phase shift to the state vector, it does not commute, in general, with the current operator \hat{I} which originates from a higher dimensional system.

III. MODEL CIRCUIT

The Cooper pair pump shown in Fig. 1(c) is considered here as the physical realization for observing non-Abelian geometric phases. It consists of three superconducting quantum interference devices (SQUIDs) in series with two superconducting islands between them. The SQUIDs are operated as tunable Josephson junctions which can be closed (Josephson energy E_j is zero) and opened ($E_j \neq 0$) by controlling the magnetic flux through them. The phase difference of the order parameter across the whole device, $\varphi = \phi_R - \phi_L$, is kept constant by the magnetic flux Φ through the outermost loop. The Hamiltonian has five external parameters which are controlled during a pumping cycle, i.e., three magnetic fluxes and two gate voltages.

The charging energy part of the Hamiltonian, H_{ch} , is given by

$$H_{\text{ch}} = E_{C_1}(\hat{n}_1 - n_{g1})^2 + E_{C_2}(\hat{n}_2 - n_{g2})^2 + E_m(\hat{n}_1 - n_{g1})(\hat{n}_2 - n_{g2}), \quad (4)$$

where \hat{n}_i is the operator for the excess number of Cooper pairs on the i th island and n_{gi} is the corresponding gate charge given by $n_{gi} = C_{gi}V_{gi}/(2e)$. The charging energies are

$E_{C_1} = 2e^2 C_{\Sigma_2} / C^2$, $E_{C_2} = 2e^2 C_{\Sigma_1} / C^2$, and $E_m = 4e^2 C_m / C^2$. Here, C_{Σ_i} is the total capacitance of the i th island and $C^2 = C_{\Sigma_1} C_{\Sigma_2} - C_m^2$.

The Josephson part of the Hamiltonian, H_J , reads

$$H_J = \sum_{n_1, n_2 = -\infty}^{\infty} (J_{\text{eff},1} |n_1 + 1, n_2\rangle \langle n_1, n_2| + J_{\text{eff},m} |n_1 + 1, n_2 - 1\rangle \times \langle n_1, n_2| + J_{\text{eff},2} |n_1, n_2 + 1\rangle \langle n_1, n_2| + \text{H.c.}), \quad (5)$$

where $|n_1, n_2\rangle$ denotes the state with n_i excess Cooper pairs on the i th island, $J_{\text{eff},1} = -E_1(\Phi_1)e^{i\varphi(\Phi)/2}/2$, $J_{\text{eff},2} = -E_2(\Phi_2)e^{-i\varphi(\Phi)/2}/2$, and $J_{\text{eff},m} = -E_m(\Phi_m)/2$. Here, E_1 , E_2 , and E_m are the tunable Josephson energies. The full Hamiltonian is given by $H = H_{\text{ch}}(V_{g1}, V_{g2}) + H_J(\Phi_1, \Phi_2, \Phi_m, \Phi)$.

IV. NON-ABELIAN CYCLE

If all the SQUIDs are closed, the conventional stability diagram with a hexagonal structure is recovered,²³ see Fig. 2. In the vicinity of the triple degeneracy point of states $|1, 0\rangle$, $|0, 1\rangle$, and $|1, 1\rangle$, the adiabatic evolution is approximately restricted to these three states. The parameter cycle is composed of three symmetric paths in each of which a SQUID is opened, the gate voltages are shifted along a ground state degeneracy, and finally the SQUID is closed.

Along each path, the effective three-level Hamiltonian has a 2×2 block and can be written as $H_{\text{eff}} = \vec{\sigma}_{i,j} \cdot \vec{B}(t) + \epsilon_k(t)|k\rangle \langle k|$, where $\vec{\sigma}_{i,j} = \{\sigma_{i,j}^x, \sigma_{i,j}^y, \sigma_{i,j}^z\}$ is a vector composed of the Pauli matrices for the states i, j (for example, $\sigma_{i,j}^x = |i\rangle \langle j| + |j\rangle \langle i|$), $\vec{B}(t)$ is an effective magnetic field, ϵ_k is the eigenvalue of the third charge state, and $\{|i\rangle, |j\rangle, |k\rangle\} = \{|1, 0\rangle, |0, 1\rangle, |1, 1\rangle\}$.

The condition of the ground state double degeneracy is satisfied by tuning the smaller eigenvalue of the 2×2 block of H_{eff} to be equal to $\epsilon_k(t)$ along the evolution. In the three-level approximation this implies that the degenerate gate-voltage paths are hyperbolas in the gate-voltage plane with only a single SQUID kept open. Along the opening and closing of the SQUIDs, we choose to change voltages linearly with the SQUID energies. In this way, a nontrivial loop encircling the triple degeneracy point can be traversed along a path with a doubly degenerate ground state.

Using the eigenstates along the three paths, we can construct a continuous global basis (defined in the whole parameter space) and calculate the connection $[\Gamma(t)]_{\alpha\beta}$. If the SQUIDs can be perfectly closed, the supercurrent due to the dynamic phase in Eq. (3) vanishes since the energies of the eigenstates do not depend on φ . In this case, the transferred charge has only a geometric contribution which can be calculated analytically from the φ dependence of the $U_{\text{geo}}(T)$ operator. For a cycle starting from the degeneracy line between the states $|1, 0\rangle$ and $|0, 1\rangle$, this yields for the geometric transformation

$$U_{\text{geo}}(T) = \begin{bmatrix} 0 & e^{i\varphi} \\ 1 & 0 \end{bmatrix}, \quad (6)$$

represented in the basis $\{|1, 0\rangle, |0, 1\rangle\}$. This result was confirmed by solving numerically the Schrödinger equation us-

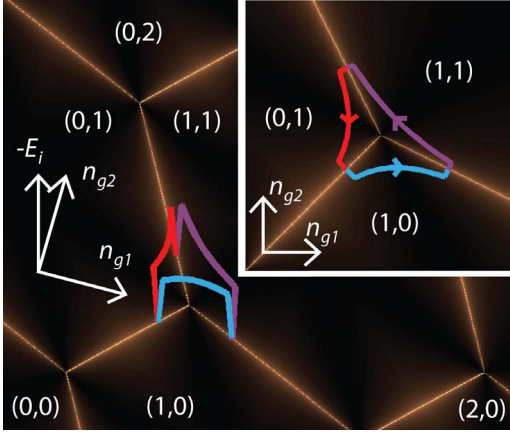


FIG. 2. (Color online) Parameter cycle inducing non-Abelian transformations with the stability diagram as the background. The charge state $|i, j\rangle$ which minimizes the charging energy in each hexagonal area is denoted by (i, j) . The z axis represents E_i with blue in the front for E_1 , purple on the right for E_m , and red on the left for E_2 . The SQUID energies can be closed down to E_i^{\min} , which is zero in the ideal cycle. The inset shows the parameter cycle projected into the gate-voltage plane.

ing 25 charge states indicating that our analysis does not rely on the three-state approximation. The obtained transformation is topological in the sense that it does not depend on the exact values to which the SQUIDs are opened as long as the evolution is kept degenerate along the cycle. From Eq. (3), we obtain for the geometrically pumped charge

$$Q = 2e[c_1^*(0), c_2^*(0)] \begin{bmatrix} 0 & 0 \\ 0 & 1 \end{bmatrix} \begin{bmatrix} c_1(0) \\ c_2(0) \end{bmatrix} = 2e|c_2(0)|^2. \quad (7)$$

Thus, the pumped geometric charge is independent of the phase across the device and depends only on the initial state.

V. OBSERVATION SCHEME FOR NON-ABELIAN PHASES

Here we discuss two methods to observe the non-Abelian transformations. First, a single-electron transistor (SET) can be coupled asymmetrically to the superconducting islands and used as a charge sensor. The additional capacitance due to the SET changes slightly the charging energies but does not affect the operation principle of the circuit. Initializing the system and performing the parameter cycle adiabatically swaps the charge states of the islands regardless of the phase across the device, which can be detected with the charge sensor. Observation of this charge transfer proves the non-Abelian character of the evolution since in the Abelian case, initial populations are conserved in cyclic adiabatic evolutions.

Another way to observe the non-Abelian features is to measure the pumped charge through the system using a detector junction.²² Since in the experiments the SQUIDs cannot be perfectly closed,^{15,24} we consider here a case in which the Josephson energies can be tuned down to E_i^{\min} of their maximum value E_i^{\max} .

In the case of nonideal SQUIDs, two additional effects have to be considered. First, the supercurrent contribution

usually dominates over the geometric contribution. However, it has been shown²² that the supercurrent contribution can be efficiently measured by traversing the parameter cycle first forward and then backward. In the perfect adiabatic limit, the geometric component of the current cancels itself and the measured total current is twice the supercurrent.

Second, the two lowest energy eigenstates are not perfectly degenerate but have an energy gap $\delta \sim E_i^{\min}$, see Fig. 1(b). To obtain non-Abelian evolution, the loop has to be traversed fast enough such that the two lowest eigenstates are effectively degenerate, that is $T \ll \hbar/\delta$, where T is the cycle period. On the other hand, the evolution should be slow enough to avoid transitions to the higher states implying $T \gg \hbar/\Delta$, where Δ is the energy gap to the excited state. To obtain the Abelian limit, the energy gap δ can be increased by larger Josephson energies and the cycle can be traversed slower such that no transitions occur.

The system can be initialized to the state $|1, 0\rangle$ by the following procedure. First, all the SQUIDs are closed to E_i^{\min} and gate voltages tuned to have $|1, 0\rangle$ as a nondegenerate ground state. After the system has relaxed to the ground state, the gate voltages are suddenly shifted, $T_{\text{shift}} \ll \hbar/\delta$, to the degeneracy line between the states $|1, 0\rangle$ and $|0, 1\rangle$. The sudden shift keeps the system in the state $|1, 0\rangle$ and the non-Abelian cycle can be traversed starting from a well-known initial state. The system can be initialized to the state $|0, 1\rangle$ with a similar procedure.

To describe the adiabaticity of the evolution, we introduce the adiabaticity parameter α defined as the population of the initial state after a back and forth cycle. In the perfectly non-Abelian regime, the geometric transformations induced by the forward and backward cycles exactly cancel each other. Thus, the total transformation is proportional to the identity implying that $\alpha=1$. For the perfectly Abelian limit, no transitions occur between the eigenstates and again $\alpha=1$ if the initial state is an eigenstate. Between these two regimes, no easy theoretical prediction can be made since the states are only partially mixed during the evolution.

In all numerical simulations, we fix the phase across the device φ to zero and $E_{C_i}=0.2$ meV. Figure 3(a) suggests that for non-Abelian cycle with period $5 \leq T \leq 10$ ns the evolution is adiabatic and α is close to unity even if the SQUIDs cannot be perfectly closed with $k=E_i^{\max}/E_i^{\min}=1000$. In this regime, the pumped charge shown in Fig. 3(b) reaches the value $2e$ or 0 depending on the initial state as predicted by Eq. (7). With $k=5000$ the adiabatic evolution window is broad and observed as a pumped charge plateau. To obtain a measurable current with a reasonable averaging time (>1 pA),²² the pumping cycle needs to be repeated fast enough. If simply a sequence of repeated pumping cycles is performed, the measured current reflects the average pumped charge e regardless of the initial state due to the swapping between the states $|0, 1\rangle$ and $|1, 0\rangle$. On the contrary, the system can be initialized to the same state before every cycle. In this case, the pumped charge per cycle is $2e$ or 0 depending on the initial state. Measuring such dependence on the initialization indicates that the charge states are swapped after each cycle providing a fingerprint of the non-Abelian evolution.

The evolution can be made Abelian by increasing the cycle period and keeping all the SQUIDs constantly open

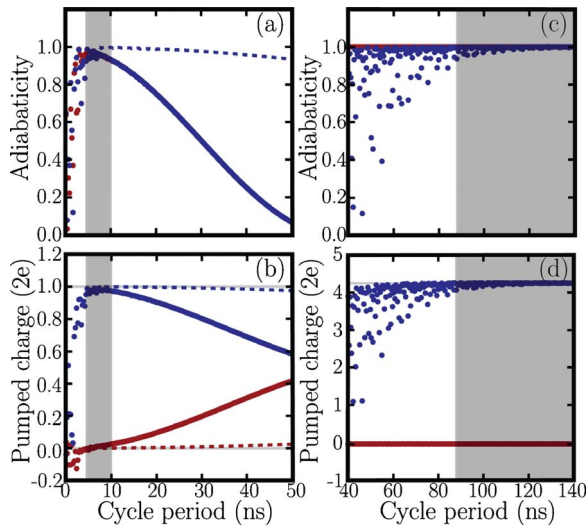


FIG. 3. (Color online) (a) Adiabaticity as a function of the cycle period in a cycle with $E_i^{\max} = -0.4E_C$ and $E_i^{\min} = E_i^{\max}/k$. Red (blue) denotes a cycle starting from the initial state $|1,0\rangle$ ($|0,1\rangle$) for $k = 1000$ (dots) and $k = 5000$ (dashed line). (b) The pumped charges corresponding to (a). (c) Adiabaticity of the ground (red) and excited states (blue) in a cycle with all the SQUID energies fixed to $E_i^{\max} = E_i^{\min} = -0.4E_C$. (d) The pumped charges corresponding to (c). In (b) and (d) the gray lines denote the geometric pumped charges in the perfectly adiabatic limits. The shaded areas indicate the cycle periods with which the evolution is adiabatic. The charging energy E_C used is experimentally realizable 0.2 meV (Ref. 22) and the phase across the device is fixed to zero, $\varphi = 0$.

with $E_i^{\max} = E_i^{\min} = -0.4E_C$. Figure 3(c) indicates that the evolution is adiabatic with cycle periods longer than ~ 85 ns and additional results (not shown here) confirm that the evolution is Abelian. Numerical simulations for the pumped charge, shown in Fig. 3(d), yield $8.5e$ or 0 depending on the initial state which are the two lowest eigenstates. The pumped charge in the Abelian limit depends on φ which in the simulation is fixed to zero. Here, the two different procedures (with and without initialization between the pumping cycles) lead to the same average pumped charge pointing out that no swapping between the lowest eigenstates takes place.

In conclusion, we have presented a rather simple superconducting circuit with which non-Abelian geometric transformations can be realized in the ground state of the system. A parameter cycle is introduced for which the corresponding geometric transformation is determined analytically. Two observation schemes are presented for the non-Abelian features taking into account the most important experimental restrictions.

ACKNOWLEDGMENTS

The authors thank V. Pietilä for insightful discussions. This work is supported by Academy of Finland, Emil Aaltonen Foundation, and Finnish Cultural Foundation. This work was partially funded by the Australian Research Council, the Australian Government, the U.S. National Security Agency, the U.S. Army Research Office under Contract No. W911NF-04-1-0290, and European Community's Seventh Framework Programme under Grant Agreement No. 238345 (GEOMDISS).

- ¹J. Anandan, J. Christian, and K. Wanelik, *Am. J. Phys.* **65**, 180 (1997).
- ²J. Pekola, V. Brosco, M. Möttönen, P. Solinas, and A. Shnirman, [arXiv:0911.3750](https://arxiv.org/abs/0911.3750) (unpublished).
- ³M. V. Berry, *Proc. R. Soc. London, Ser. A* **392**, 45 (1984).
- ⁴B. Simon, *Phys. Rev. Lett.* **51**, 2167 (1983).
- ⁵F. Wilczek and A. Zee, *Phys. Rev. Lett.* **52**, 2111 (1984).
- ⁶P. Zanardi and M. Rasetti, *Phys. Lett. A* **264**, 94 (1999).
- ⁷J. A. Jones, V. Vedral, A. Ekert, and G. Castagnoli, *Nature (London)* **403**, 869 (2000).
- ⁸J. J. L. Morton, A. M. Tyryshkin, A. Ardavan, S. C. Benjamin, K. Porfyarakis, S. A. Lyon, G. Andrew, and D. Briggs, *Nat. Phys.* **2**, 40 (2006).
- ⁹Y. Aharonov and J. Anandan, *Phys. Rev. Lett.* **58**, 1593 (1987).
- ¹⁰R. G. Unanyan, B. W. Shore, and K. Bergmann, *Phys. Rev. A* **59**, 2910 (1999).
- ¹¹L.-M. Duan, J. I. Cirac, and P. Zoller, *Science* **292**, 1695 (2001).
- ¹²I. Fuentes-Guridi, J. Pachos, S. Bose, V. Vedral, and S. Choi, *Phys. Rev. A* **66**, 022102 (2002).
- ¹³A. Recati, T. Calarco, P. Zanardi, J. I. Cirac, and P. Zoller, *Phys. Rev. A* **66**, 032309 (2002).
- ¹⁴P. Solinas, P. Zanardi, N. Zanghi, and F. Rossi, *Phys. Rev. B* **67**, 121307(R) (2003).
- ¹⁵L. Faoro, J. Siewert, and R. Fazio, *Phys. Rev. Lett.* **90**, 028301 (2003).
- ¹⁶M.-S. Choi, *J. Phys.: Condens. Matter* **15**, 7823 (2003).
- ¹⁷V. Brosco, R. Fazio, F. W. J. Hekking, and A. Joye, *Phys. Rev. Lett.* **100**, 027002 (2008).
- ¹⁸J. P. Pekola, J. J. Toppari, M. Aunola, M. T. Savolainen, and D. V. Averin, *Phys. Rev. B* **60**, R9931 (1999).
- ¹⁹M. Aunola and J. J. Toppari, *Phys. Rev. B* **68**, 020502(R) (2003).
- ²⁰M. Möttönen, J. P. Pekola, J. J. Vartiainen, V. Brosco, and F. W. J. Hekking, *Phys. Rev. B* **73**, 214523 (2006).
- ²¹P. J. Leek, J. M. Fink, A. Blais, R. Bianchetti, M. Göppl, J. M. Gambetta, D. I. Schuster, L. Frunzio, R. J. Schoelkopf, and A. Wallraff, *Science* **318**, 1889 (2007).
- ²²M. Möttönen, J. J. Vartiainen, and J. P. Pekola, *Phys. Rev. Lett.* **100**, 177201 (2008).
- ²³R. Leone and L. Lévy, *Phys. Rev. B* **77**, 064524 (2008).
- ²⁴A. Kemppinen, A. J. Manninen, M. Möttönen, J. J. Vartiainen, J. T. Peltonen, and J. P. Pekola, *Appl. Phys. Lett.* **92**, 052110 (2008).